SSRG International Journal of Electrical and Electronics Engineering
ISSN: 2348-8379/ https://doi.org/10.14445/23488379/IJEEE-V11I2P106

Volume 11 Issue 2, 47-57, February 2024

Original Article

Modelling and Simulation of UWB Channel for Indoor Localization System

Sujata Mohanty[1], Aruna Tripathy[2], Bikramaditya Das[3]

[1]*Department of Electronics and Telecommunication Engineering, Biju Patnaik University of Technology (BPUT), Odisha, India.*
[2]*School of Electronic Sciences, Odisha University of Technology and Research, Odisha, India.*
[3]*Department of Electronics and Telecommunication Engineering, VSS University of Technology, Odisha, India.*

[1]*Corresponding Author : sujatamohanty1988@gmail.com*

Received: 16 November 2023 Revised: 06 December 2023 Accepted: 16 January 2024 Published: 16 February 2024

Abstract *- Localization is the most important and interesting area for research work in wireless networking systems. Indoor Localization System (ILS) with UWB signal dispenses precise and real-time positioning of any target node or person within an indoor area system. This system determines the location of the target in a particular indoor environment constantly and on a time basis with the actual time mode of operation. There are different applications in indoor area systems such as in shopping malls, In the military, in the health care system, museums, in IOT, etc. It is very requisite to find a definite and reliable channel model for UWB localization in ILS. The IEEE 802.15.3a standardization is meant for the UWB indoor channel model for Wireless PAN, which offers low cost with less consumption of power along with high data rate to WPAN devices. The operation of localization is carried out using two steps: ranging and positioning. With these two steps, the distance value (between label and base stations) and the coordinate value of the target point are evaluated, respectively. The multipath fading model adapted in The IEEE802.15.3a standard is based upon the Saleh- Valenzuela (S-V) model through a couple of modifications. According to the path amplitude distribution, the different models for channel parameters can be given as Rayleigh distribution, Ricean distribution, Log normal distribution, etc. The S-V model suggested Rayleigh distribution in favor of multipath gain magnitude. This paper includes the modified S-V model, which is applied for the simulation of different UWB channel models that are CM-1, CM-2, CM-3, and CM-4. It also includes the UWB simulation system, which undergoes averaging and correlation of the received UWB signal with the original transmitted UWB signal to find the ToA data to locate the target in an indoor area system. The operation is carried out in CM-2, which corresponds to the S-V model with Rayleigh distribution in a typical indoor scenario.*

Keywords *- Localization, ILS, WPAN, LOS, NLOS.*

1. Introduction

In the field of localization, UWB plays a vital role for its different features, such as a high spectrum that is 7.5GHz, less duty cycle, high ranging accuracy (cm), small pulses (ns), high penetrating capacity, less multipath fading, etc. The Federal Communications Commission (FCC) has allocated the spectrum (3.1 GHz - 10.6 GHz) that is unlicensed for indoor UWB operation and defined this signal with -10 dB bandwidth, which is higher than 500 MHz [1-4].

The signal paths from the transmitter to the receivers are referred to as radio channels. This radio channel is random by nature; hence, the received signals are destructive or constructive by nature at the side of the receiver. This is called fading. This multipath fading generates limitations in the output behaviour of signal propagation through the wireless channel; hence, it is very crucial for the characterization of the wireless channel before the signal propagation through the wireless system. The IEEE 802.15.3a task group has created a physical layer for the UWB technique to support the high data rates in Wireless Personal Area Networks (WPANs).

Communications with high data rates can be gained by increasing the signal bandwidth. Nowadays, Ultra-Wideband (UWB) communications have increased attention for their capability to provide low cost along with high data rate and less power consumption of operation in the field of localization [5-7].

UWB transmits the pulses; then, it will again reflect through the doors and various obstacles with a more limited carrier signal through a broad spectrum. It creates no interference, and the regulatory bodies are moving forward cautiously; hence, the users who already have spectrum allocation are not affected. The accuracy of wireless ranging applications is very high due to the high data rate of

communication, less energy consumption, and immunity to the multipath-resistant property of the UWB system [8, 9].

The estimation of position needs channel impulse response, which can be derived in the time domain by exciting the channel through narrow pulses, or the frequency domain can also acquire it through the application of IFFT to the transfer function, which is calculated in the frequency domain. The calculation of Channel Impulse Response (CIR) in the time domain is more advantageous than that of the frequency domain since the response measurement of the channel is very fast in time domain operation [10]. The IEEE 802.15.3a standardization is meant for the UWB indoor channel model for Wireless PAN. This TG offers low cost with less power consumption.

The multipath fading model adapted in IEEE802.15.3a standard is based upon the S-V model through a couple of modifications. S-V model has proposed the Rayleigh distribution for the sake of multipath gain magnitude [11-13]. The model of propagation is categorized into two types: large-scale and small-scale propagation model. The model, that is, a large scale, refers to the signal power over significant distance separation in transmitter and receiver compared to the wavelength of the transmitted signal and is described through the path loss model and shadow effect.

The small-scale models refer to the occurrence of fluctuation in amplitudes, phases, and delays due to multipath found in the received signal within a very short time period and a very small distance apart (a few meters inside the indoor area). Generally, fading occurs due to path loss, and the shadow effect is common for all types of environments. Still, the fading occurs due to multipath varying according to the kind of environment. The major issue of channel modeling is multipath fading [14, 15].

This paper includes the IEEE 802.15.3a standard TG, which is the S-V channel model for indoor UWB localization. It also consists of the limitations and modifications to the S-V model along with different model parameters to UWB channel in the area of positioning. The four different types of indoor Channel Models (CM-1, CM-2, CM-3, and CM-4) have also been simulated using Matlab. It also includes the UWB system model, which undergoes the operation of averaging and correlating the received UWB signal with the original transmitted UWB signal to find the ToA information to locate the location of the target in ILS.

This operation is carried out in CM2, which corresponds to the S-V model with Rayleigh distribution in the area of localization. All the reported work in the literature assumes a particular channel model to perform localization. However, this work determines the channel type from the ToA information as obtained through averaging and correlation before carrying out localization.

This paper includes five sections. Following the introduction, section 2 contains related work, which gives an overview of the UWB channel model, that is, the Saleh-Valenzuela channel model, along with its limitations and modifications in the area of the localization system. Section 3 discusses the system model used to identify the Time of Arrival (ToA) value, which can be used to get the coordinates of the target node in the field of localization. Section 4 provides the simulation results for four different types of indoor channel models, along with a simulation of the UWB system for getting the ToA information. Section 5 includes the conclusion and the proposed work, which can be studied further.

2. Related Works

The UWB technology behaves as a leading-edge technique for low-range and high-data-rate wireless communication systems. The communication due to the UWB system can be defined as whose instantaneous bandwidth is many times more than that of the required information to be delivered in the indoor system. The different location detection techniques are proximity type and triangulation type. Proximity is a technique of connectivity; though this method is straightforward, it produces less accuracy [16].

The triangulation type is based on direction-based and distance-based methods of operation. The triangulation type uses the property of the geometry of the triangle to find the location of the target. Again, there are two types: lateration and angulation [17]. The different techniques that are based on propagation time are TOA, TDOA, and RTOF. The lateration method depends on propagation time. Lateration determines the location of the target by calculating the distance from the reference points, which is known as the based measurement technique. Different techniques are present in the lateration method, such as TOA, RTOF, and TDOA.

The multipath fading model is the central issue of channel modeling in the area of the indoor UWB localization system [18-21]. The UWB channel model can be generated through the S-V model. A signal propagation experiment is carried out through the indoor office area for the characterization of the UWB channel, but in the output, it is found that the channel operates very slowly with time; hence, the modification in the S-V model is required, and then examined for simulating the channel. The result found that it is appropriate for both LOS and NLOS with proper delay in observed value [22].

The UWB channel model can also be carried out through a deterministic method of operation, which requires geometric information to conduct the operation. Different methods exist for canceling out the MPC effect to get better accuracy in generating the UWB channel model in Iindoor. The different parameters of the UWB S-V model can be calculated by conducting measurements using different measured data.

There are different methods available for measuring the channel band of UWB, and a control chain can be used to find the interfering signals in the signal transmission while conducting UWB localization [24]. The positioning behavior of UWB Channel Impulse Responses (CIRS) and an appropriate technique can also be used for localizing the target in a complex propagation region like the Industrial area of localization.

A modified S-V model is investigated for the ultra-high frequency band of operation, and it is operated in a large exhibition hall for the generation of an indoor channel model conducted in a LOS area of investigation and also performed on a new cognitive radio system. It is found that the path of the signal through the Rayleigh distribution function will provide more accurate average power within a cluster of signal propagation [25].

The data rate of the IR-UWB system can also be implemented by using the modulation that is Orthogonal Amplitude Modulation (OAM) technique. Then, finally, the rake receiver is used at the receiver to improve the accuracy of the system performance [26].

The outcome of the system in an indoor wireless channel can also be evaluated on the basis of approximation of the captured energy over the wireless channel through coaxian, gamma mixture, or lognormal distribution function by least square fitting property and the BER of the system is found out [27].

A modified S-V channel model is found to compensate for low data rate communication in under water communication systems. Here, the Rician distribution is used in MPC gain in the UWB channel through the underwater communication system. The range is examined through communication in underwater systems on the basis of different time dispersion parameters [28].

In this paper, an attempt has been made to i) estimate the ToA of a UWB pulse by performing a simple averaging and correlation at the receiver, and ii) this value is used to identify the type of channel that the device is operating in.

2.1. UWB Channel Model

The IEEE 802.15.3a standardization is meant for the UWB indoor channel model for Wireless PAN, which offers low cost with less consumption of power along with high data rate to WPAN devices. The major issue of channel modeling is multipath fading [29].

The multipath fading models are given by many channel models like Δ-k model, Tap delay line, Saleh-Valenzuela model, etc. The multipath fading model adapted in IEEE802.15.3a standard is stated on the S-V model with a couple of slight modifications.

According to the path amplitude distribution, the different models for channel parameters can be given as Rayleigh distribution, Ricean distribution, Log normal distribution, etc. The S-V model proposed Rayleigh distribution in multipath gain magnitude. In the S-V model, the multipath arrivals can be categorized as arrival in a cluster and arrival in rays within a cluster.

The power of these components reduces with time. It has been modeled as an exponential power delay profile. The multipath component of the UWB channel includes many important parameters like excess delay, power decay profile, RMS delay spread, etc. [30].

2.1.1. IEEE 802.15.3a/Saleh-Valenzuela (S-V) Channel Model

The complex low pass CIR is shown by [31]:

$$H(t) = \sum_k \beta_k e^{j\theta_k} \sigma(t - \tau_k) \tag{1}$$

Where,
$\sigma(.)$ represents the dirac delta function,
β_k represents a positive gain coefficient,
τ_k represents propagation delay,
Θ_k represents associated phase shift,
k represents the path index.

The complex time domain representation of the pulse is shown by:

$$X(t) = p(t) e^{j(\omega t + \phi)} \tag{2}$$

Here,
p(t) shows the baseband of the pulse shape,
ω act as RF angular frequency,
ϕ represents the arbitrary phase,

Now the received signal, that is:

$$Y(t) = \sum_k \beta_k p(t - \tau_k) e^{j\theta_k[\omega(t-\tau_k)+\phi+\phi_k]} \tag{3}$$

Now the Power profile is shown as:

$$|Y(t)|^2 = \sum_k \sum_l \{ \beta_k p(t - \tau_k) p(t - \tau_l) e^{j[\theta_k - \theta_l + \omega(\tau_l - \tau_k)]} \} \tag{4}$$

If no overlapping of pulses occurs, then it can be represented as:

$$|Y(t)|^2 = \sum_k \beta_k{}^2 p^2(t - \tau_k) \text{ (No overlapping)} \tag{5}$$

If the swept bandwidth is very large, then

$$S(t) = \frac{1}{\Delta f}\int_{-\frac{\Delta f}{2}}^{\frac{\Delta f}{2}} |\, y(t)\,|^2 df \sum_k \beta_k{}^2 p^2\left(t-\tau_k\right) \quad (6)$$

The model includes that the rays are arriving within the clusters, and the cluster arrival time is modeled as a poisons arrival process having a fixed rate, that is Λ.

The rays that are arriving in the cluster as the Poisson process have a fixed rate, that is λ, where $\lambda << \Lambda$.

Let T_1 be time of arrival for l^{th} cluster and $\tau_{k,l}$ be time of arrival for k^{th} ray in l^{th} cluster.

Now T_0= 0, for the first cluster, and $\tau_{k,l}$ =0, is the first ray in l^{th} cluster.

The representation for the distribution of TOA of the cluster and TOA of the ray can be expressed by:

$$P(T_l/T_{L-1}) = \Lambda \exp\left[-\Lambda\left(T_l - T_{L-1}\right)\right], l > 0 \quad (7)$$

$$P\left(\tau_{k,l}/\tau_{k-1,l}\right) = \lambda \exp\left[-\lambda\left(\tau_{k,l} - \tau_{k-1,l}\right)\right], k > 0, l > 0 \quad (8)$$

Here, amplitude distribution in the S-V model was best for Rayleigh distribution, where power is coordinated and controlled through decay factors (ray, cluster).

S-V model utilizes two poison processes to define the multipath component.

Firstly, it describes the cluster arrival, and secondly, it describes the rays arrival in the cluster.

T_1 Shows the time of arrival for the first path in l^{th} cluster,

$\tau_{k,l}$ represents the delay in k^{th} path within l^{th} cluster,
Λ is the arrival rate of the cluster,
λ is the arrival rate of ray.

Now, the impulse response for Equation (1) is given by:

$$H(t) = \sum_{l=0}^{\infty}\sum_{k=0}^{\infty} \beta_{k,l} e^{j\theta_{k,l}} \sigma\left(t - T_l - \tau_{k,l}\right) \quad (9)$$

Here,
$\beta_{k,l}$ determines gain for k^{th} ray in l^{th} cluster,
$\Theta_{k,l}$ represents the phase of a statistically independent uniform random variable.

2.2. Limitations and Modifications to S-V Model

The limitations of the S-V model can be given as [32]:

1. This model provides less accuracy in the LOS area of operation.
2. It is very difficult to find the value of the arrival rate of the cluster and the exponential decay constant of the inter-cluster for the purpose of modeling the cluster behaviour on the basis of experimental data.

The limitations of the S-V model can be reduced by:

1. Considering two cluster models having two deterministic times of arrival of clusters with stochastic arriving rays. The model is purely formed on the S-V model, and the only change is it takes only two clusters for consideration rather than considering more clusters for operation.
2. The distribution of the rays in the first cluster and second cluster are represented deterministically instead of stochastically as computed in the previous S-V model. The gain of the rest of the rays of the two clusters is represented statistically.

Now, the response of the channel is shown by:

$$H(t) = \sum_{k=0}^{M-1} \alpha_{k,0}\delta\left(t-\tau_{k,0}\right) + \sum_{k=0}^{N-1} \alpha_{k,l}\delta\left(t - T_m - \tau_{k,l}\right) \quad (10)$$

Here,
$\alpha_{k,l}$ determines gain coefficient,
T_m shows interval time in between the two clusters,
$\tau_{k,0}$ represents delay for k^{th} MPC with respect to arrival of the first cluster,
$\tau_{k,l}$ represents delay for k^{th} MPC with respect to arrival (T_m)of the second cluster,
M shows the number of paths in the first cluster and N the number of paths in the second cluster.

This model includes two types of parameters, deterministic and stochastic. The deterministic part contains the path gain value for the first ray to that of two clusters, along with their delay period.

Here, the ray of LOS is taken as the first ray to that of the first cluster, whose time of arrival is taken as zero, and its gain can be represented by:

$$\alpha_{0,0} = \frac{\lambda}{4\pi d}, \lambda = \frac{c}{\sqrt{f_m}} \quad (11)$$

Here c, it represents the speed of light, f_m shows mean signal frequency, drepresents distance value in the transmitter and the receiver.

The second cluster having the first ray depends on the number of reflecting surfaces, and the arrival time can be represented as:

$$T_m = \frac{\min\{L_i\} - L_0}{c} \quad (12)$$

Where, i is the number of reflecting surfaces, L_0 represents the length for the direct path L_i and shows the size for the reflected ray.

Now, the gain of this ray due to reflection can be represented as:

$$\alpha_{0,1} = \frac{L_0}{L_0 + \min\{L\}} \times \left\{ \pm K \left[1 + \frac{2k}{1-k^2} \exp\left[(1+k) a T_m \right] \right] \right\} \quad (13)$$

Where, $k = \frac{1-k}{1+k}$ (14)

For vertical polarization, k is given as:

$$k = \frac{\sqrt{\varepsilon_r} - \cos^2 \varphi}{\varepsilon_r - \sin \varphi} \quad (15)$$

For horizontal polarization, the value of k can be written as:

$$k = \frac{\sin \varphi}{\sqrt{\varepsilon_r - \cos^2 \varphi}} \quad (16)$$

The value of a is given as:

$$a = \frac{120 \pi \sigma c}{\varepsilon_r}$$

Where, ε_r is the relative dielectric constant, σ is the conductivity of the reflecting surface.

The statistical portion of the model contains the remaining rays (instead of the first ray) in both clusters, whose gain and time of arrival can be shown statistically.

Now, the gain of the rays can be represented as:

$$\alpha_{k,0/1} = p_{k,0/1} \beta_{k,0/1}, k \geq 1 \quad (17)$$

Here $P_{k,0/1}$ represents value as ±, $\beta_{k,0/1}$ shows the lognormal fading of the rays having standard deviation δ, that is:

$$20\log(\beta_{k,0/1}) \propto Normal\left(\mu_{k,0/1}, \delta^2\right), k \geq 1$$

Finding the value of $\mu_{k,0/1}$ be conditional on the functionality of the average power delay profile in two cluster models can be represented as an exponential function:

$$E\left[\beta_{k,\,0/1}{}^2\right] = \alpha_{0,0/1}{}^2 e^{-\frac{\tau_{k,0/1}}{\nu_{0/1}}}, k \geq 1 \quad (18)$$

2.3. Model Parameters

2.3.1. Cluster Arrival Rate (Λ)

The first cluster is always present, while others may or may not be present using Poison distribution.

$$P(T_l / T_{L-1}) = \Lambda \exp\left[-\Lambda (T_l - T_{L-1}) \right], l > 0 \quad (19)$$

2.3.2. Ray Arrival Rate (λ)

Ray within clusters is also a poison process, so the distribution of interarrival time is an exponential random variable for k>0.

$$P\left(\tau_{k,l} / \tau_{k-1,l}\right) = \lambda \exp\left[-\lambda \left(\tau_{k,l} - \tau_{k-1,l}\right) \right], k > 0, l > 0 \quad (20)$$

If the time of arrival for the first cluster is the time of reference, then

$T_1^i = 0$,

$T_2^i - T_1^i = T_2^i = T_N$ (Time delay between two clusters)

So, $\tau_{0,1} = 0$ (for m=1,2)

Ray in cluster modeled as poison arrival process, so the distribution of ray within each cluster can be given as:

$$p\left(\tau_{k,m|} \mid \tau_{k-1,m}\right) = \lambda \exp\left[-\lambda \left(\tau_{k,m} - \tau_{(k-1),m}\right) \right] \quad (21)$$

The average power for both ray and cluster is supposed to be reduced exponentially; that is, the average power to that of the multipath component at a given delay $T_l = \tau_{k,l}$

$$\beta_{k,l}{}^2 = \beta_{0,0}{}^2 \exp\left(\frac{-T_l}{\nu} \right) \exp\left(\frac{-\tau_{k,l}}{\gamma} \right) \quad (22)$$

Here $\beta_{0,0}{}^2$ represents the expected value of the power of the first arrival multipath component,

ν represents the decay component of the cluster,

γ represents the decay component of rays.

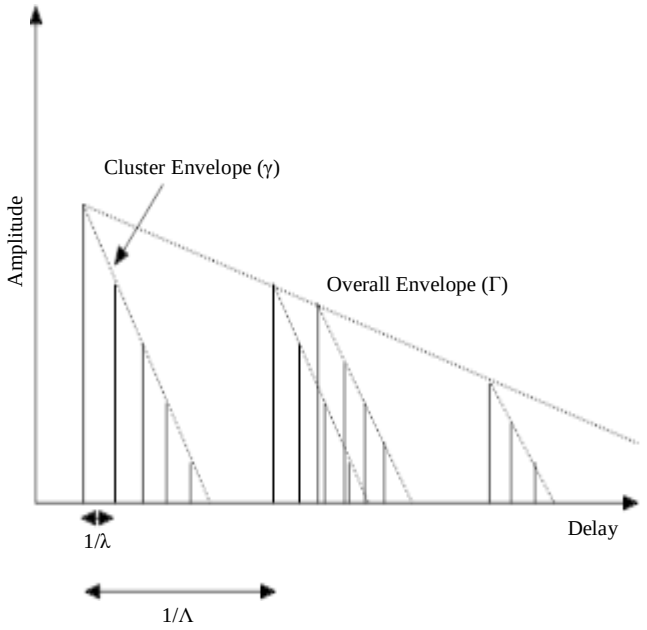

Fig. 1 Concept of S-V fading

According to the amplitude distribution, the different models for channel parameters can be given as Rayleigh distribution, Ricean distribution, Log normal distribution, etc. The Rayleigh fading area is determined by the multipath components having similar signal strength.

It has a phase with no LOS path. In this model, the communication is through Reflection and Diffraction [33]. The Rayleigh fading channel can be represented as:

$$Y_{received} = \sum_{i=1}^{N} y_i e^{j\theta_i} \tag{23}$$

It shows the addition of the Independent and Identically Distributed (IID) complex random variable. By increasing the random variable (N), the addition of two or more IID random variables seems to favor a Gaussian distribution, even as referred to by the central limit theorem of statistics. Similarly, the Rician fading can be represented by

$$Y_{received} = Y_0 + \sum_{I=1}^{N} Y_i e^{j\theta_i} \tag{24}$$

Where Y_0 represents the LOS component $\sum$ shows the aggregation of N randomly reflected path having complex amplitude y_i and the phase Θ_i.

In surviving the Rician distribution, there is Rician-K-factor is used for the presence of the dominant path in the fading channel [34].

$$\text{Rician-K-factor} = \frac{power\ in\ Losspath}{Power\ in\ reflectedpath}$$

$$K = \frac{s^2}{\sum_{i=1}^{N} \left| Y_i^{\,2} \right|} \tag{25}$$

Where, $S^2 = |Y_0^2|$

The Rician-K-factor is usually represented in dB. By increasing the K value, the strength of LOS increases, and deep fading decreases.

Similarly, when the K factor falls, there is a weak LOS with high deep fading. The IEEE 802.15.3a TG explained four categories of indoor channel models: CM1, CM2, CM3, and CM4.

The CM1 refers to the LOS area where the separation between the transmitter and receiver is below 4 meters. The CM2 model also includes a distance below 4m for the NLOS environment.

The CM3 model defines the separation of 4 to 10m for the NLOS environment. The CM4 model is meant for NLOS areas with strong delay dispersion, which causes a delay spreading with 25 ns.

The main characteristics of the channel model can be derived by using different values of 7 parameters of the channel model, which are shown below. The channel model characteristics and the parameters are listed in Table 1. The CIR of the multipath channel can be represented by:

$$H(t) = X \sum_{l=0}^{L} \sum_{m=0}^{M} \alpha_{m,l} \delta\left(t - T_l - \tau_{m,l}\right) \tag{26}$$

Here $\alpha_{m,l}$ represents the gain coefficient.

T_1 determines delay of l^{th} cluster, $\tau_{m,l}$ shows delay of m^{th} multipath component, X shows lognormal shadowing L, determines the cluster number, M determines the number of multipath components in each cluster.

From the above multipath model, we can see that the model has seven parameters that define the model entirely. The parameters are:

- Λ - Arrival rate of the cluster,
- λ - Arrival rate of the ray,
- Γ - The decay factor of the cluster,
- γ - The decay factor of Ray,
- σ_1 - Standard deviation of the cluster (in dB),
- σ_2 - Standard deviation of ray (in dB),
- σ_x - Standard deviation for total multipath realization (in dB)

3. Proposed System Model for ToA Estimation

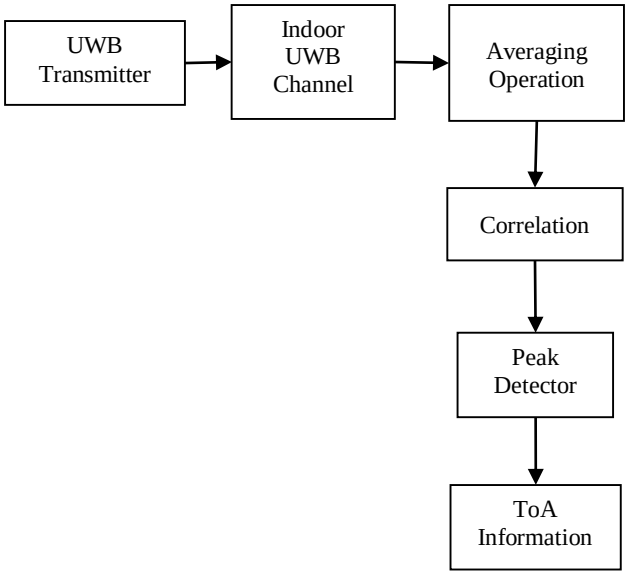

Fig. 2 Block diagram of UWB simulation system [35]

Here, in Figure 2, the UWB transmitter broadcasts short Gaussian pulses, which are passed through an indoor area channel. At the receiver side, it gets the transmitted Gaussian signal with the addition of noise.

In order to nullify the noise at the receiver section, the averaging operation is done, and then it is entered through the block of correlation. After this, the correlation is made between the received signal and that of the referenced signal.

Finally, the resulting output is entered into the peak detector, which finds the value regarding the TOA of the UWB signal for positioning in ILS. The different parameters for UWB simulation are given in Table 2. The simulation is performed using MATLAB. This overall UWB simulation process is shown in Figures 7 to 12.

4. Simulated Result

Here, in the given simulation, the occurrence of peak detection is at 700 numbers of samples. 700 samples correspond to a ToA of 11.66 ns. This results in a range of 3.5m. These results compare to a channel type primarily of the CM2 type that has mainly a Rayleigh distributed gain function. The obtained ranging information is used to find out the coordinates of the target node in ILS.

Table 1. Channel model parameters

Model Parameters	**CM1**	**CM2**	**CM3**	**CM4**
Cluster Arrival Rate Λ $(ns)^{-1}$	0.0233	0.4	0.0667	0.0667
Ray Arrival Rate λ (ns)-1	2.5	0.5	2.1	2.1
Cluster Decay Factor Γ	7.1	5.5	14	24
Cluster Decay Factor γ	4.3	6.7	7.9	12
σ_1 (dB)	3.4	3.4	3.4	3.4
σ_2 (dB)	3.4	3.4	3.4	3.4
σ_x (dB)	3	3	3	3
$E\{\|H(k)\|^2\}$	1.269	1.269	1.269	1.269
Model Characteristics				
Mean Excess Delay (nsec)	5.05	10.38	14.18	-
RMS Delay (nsec)	5.28	8.03	14.28	25
NB 10 dB	-	-	35	-
NP (85%)	24	36.1	61.54	-

Table 2. UWB simulation parameters

Simulation Parameters for UWB	Value
Speed of Light	3×10^{8} m/s
Shape of Pulse	Gaussian
SNR	30dB
Sample Rate	60GHz
Width of Pulse	0.5ns
Number of Samples	1000
Variance	0.2

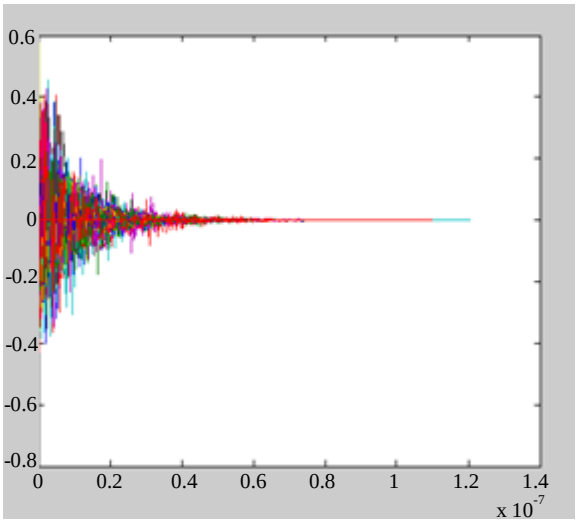

Fig. 3 Impulse respose for CM-1 channel

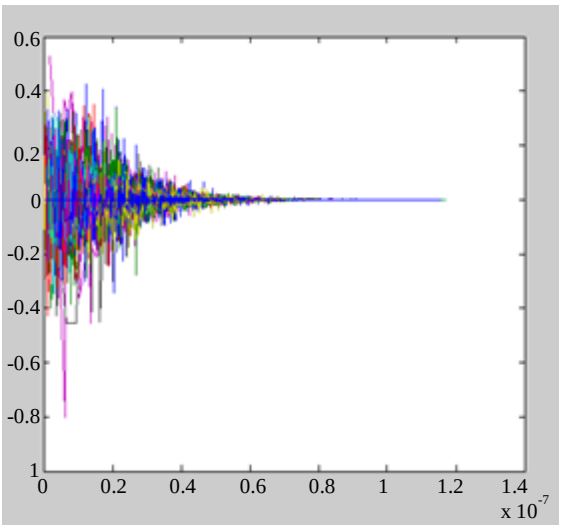

Fig. 4 Impulse respose for CM-2 channel

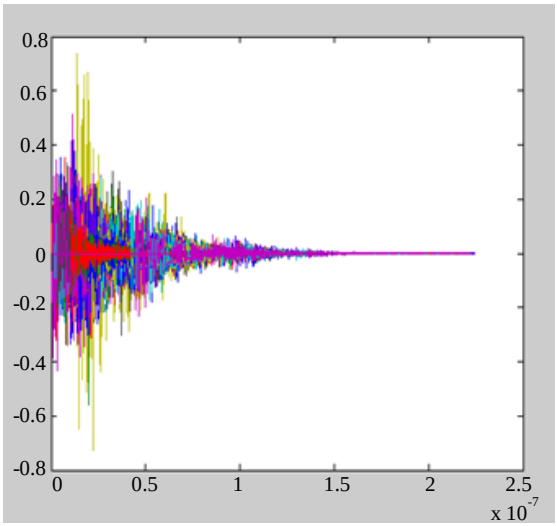

Fig. 5 Impulse respose for CM-3 channel

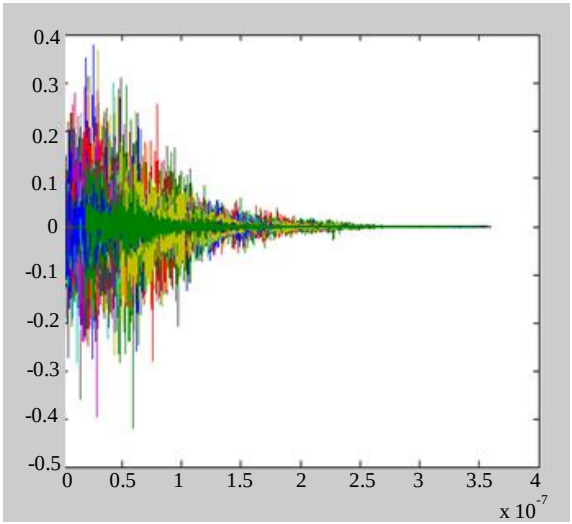

Fig. 6 Impulse respose for CM-4 channel

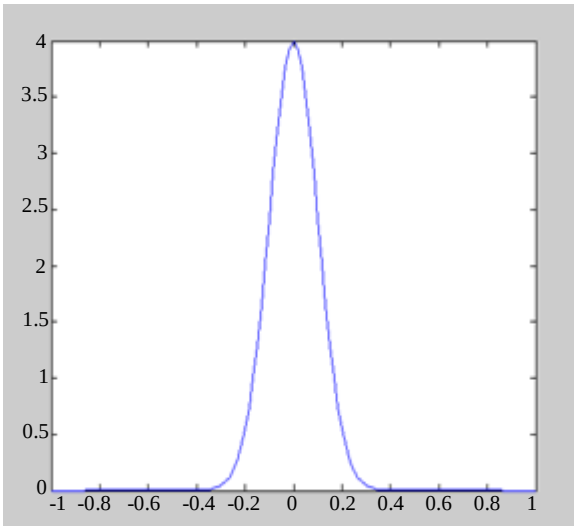

Fig. 7 Gaussian pulse signal

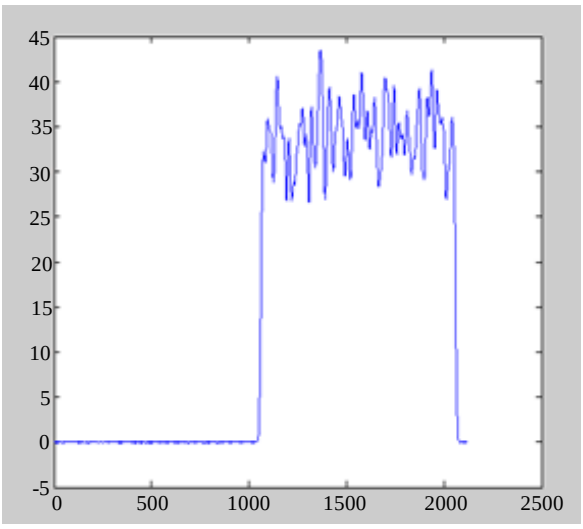

Fig. 10 Delayed signal with noise

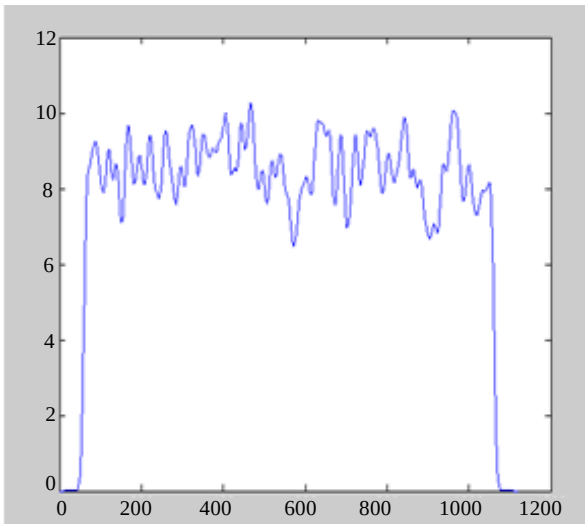

Fig. 8 Convolution of UWB with channel

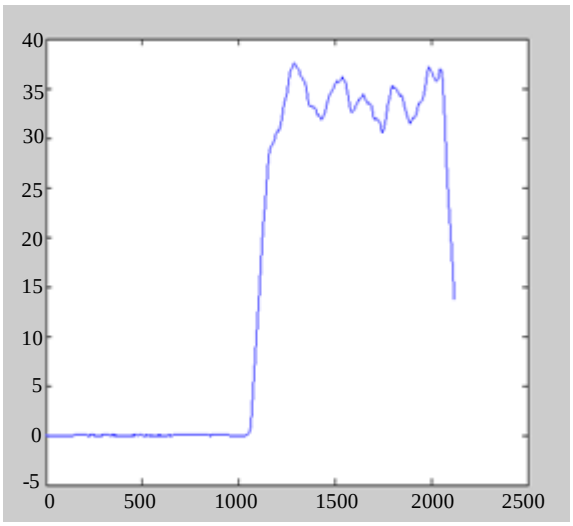

Fig. 11 Averaging output signal

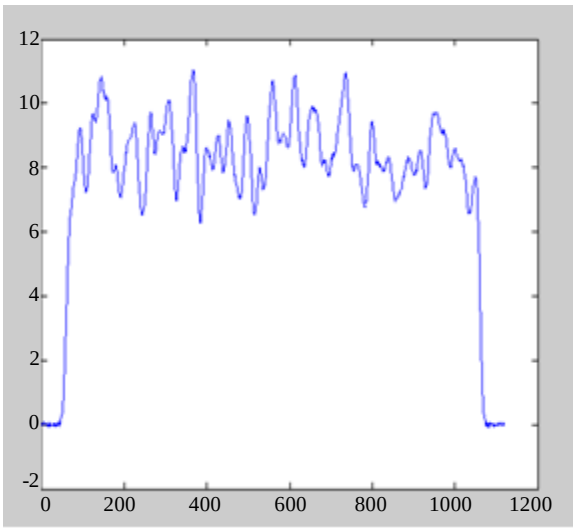

Fig. 9 Signal added with noise

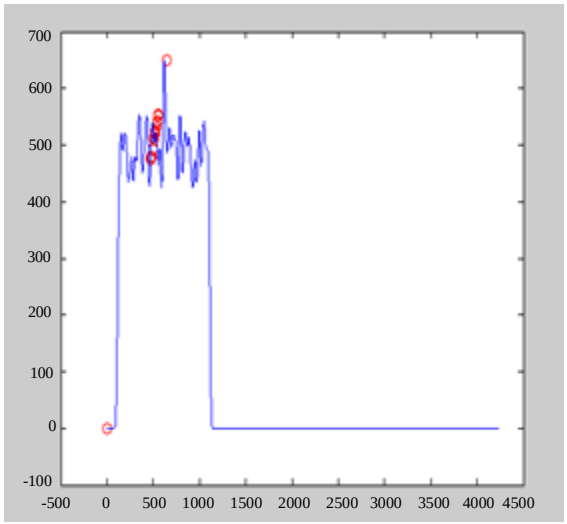

Fig. 12 Correlated output signal with peak detection

5. Conclusion and Future Scope

The channel model parameters and different characteristics of all four types of channel models are listed in Table 1, and the impulse response of four channels is shown in Figures 3 to 6 using MATLAB simulation. From these simulated results, it is observed that the occurrence of clutter increases with the increase of distance and existence of NLOS in channel models, that is, CM1 to CM4. It is also found that the presence of AWGN in the transmitted UWB signal can be nullified by passing it through the averaging operation, and the correlation is done at the receiver between the received signal and that of the reference signal to find out the ToA information, which will help in locating the target position in the area of indoor localization.

References

[1] Sixto Campaña-Bastidas, Macarena Espinilla-Estévez, and Javier Medina-Quero, "Review of Ultra Wideband for Indoor Positioning with Application to Elderly," *Proceedings of 55th Hawali International Conference on System Science*, pp. 2145-2154, 2022. [Google Scholar] [Publisher Link]

[2] Laura Flueratoru et al., "On the Energy Consumption and Ranging Accuracy of Ultra Wide Band Physical Interfaces," *GLOBECOM 2020 - 2020 IEEE Global Communications Conference*, Taipei, Taiwan, pp. 1-7, 2020. [CrossRef] [Google Scholar] [Publisher Link]

[3] Faheem Zafari, Athanasios Gkelias, and Kin K. Leung, "A Survey of Indoor Localization Systems and Technology," *IEEE Communications Surveys and Tutorials*, vol. 21, no. 3, pp. 2568-2599, 2019. [CrossRef] [Google Scholar] [Publisher Link]

[4] B. Venkata Krishnaveni, K. Suresh Reddy, and P. Ramana Reddy, "Wireless Indoor Positioning Techniques Based on Ultra Wideband Technology," *International Journal of Recent Technology and Engineering (IJRTE)*, vol. 7, no. 5C, pp. 15-22, 2019. [Google Scholar] [Publisher Link]

[5] Yuankang Gao et al., "UWB Systems and Algorithms for Indoor positioning," *2021 Telecoms Conference (ConfTELE)*, Leiria, Portugal, pp. 1-6, 2021. [CrossRef] [Google Scholar] [Publisher Link]

[6] Abdulrahman Alarifi et al., "Ultra Wide Band Indoor Positioning Technologies Analysis and Recent Advances," *Sensors*, vol. 16, no. 5, pp. 1-36, 2016. [CrossRef] [Google Scholar] [Publisher Link]

[7] W. Pam Siriwongpairat, and K.J. Ray Liu, *Ultra-Wideband Communications Systems: Multiband OFDM Approach*, Wiley-IEEE Press, pp. 1-248, 2007. [Google Scholar] [Publisher Link]

[8] N. Syazwani C.J. et al., "Indoor Positioning System: A Review," *International Journal of Advanced Computer Science and Applications*, vol. 13, no. 6, pp. 477-490, 2022. [CrossRef] [Google Scholar] [Publisher Link]

[9] Huthaifa Obeidat et al., "A Review of Indoor Localization Techniques and Wireless Technologies," *Wireless Personal Communications*, vol. 119, pp. 289-327, 2021. [CrossRef] [Google Scholar] [Publisher Link]

[10] Sebastian Kram et al., "UWB Channel Impulse Responses for Positioning in Complex Environments: A Detailed Feature Analysis," *Sensors*, vol. 19, no. 24, pp. 1-26, 2019. [CrossRef] [Google Scholar] [Publisher Link]

[11] A.F. Molisch, J.R. Foerster, and M. Pendergrass, "Channel Models for Ultra Wideband Personal Area Networks," *IEEE Wireless Communications*, vol. 10, no. 6, pp. 14-21, 2003. [CrossRef] [Google Scholar] [Publisher Link]

[12] Tarik Kazaz et al., "Delay Estimation for Ranging and Localization Using Multiband Channel State Information," *IEEE Transaction on Wireless Communications*, vol. 21, no. 4, pp. 2591-2607, 2022. [CrossRef] [Google Scholar] [Publisher Link]

[13] J. Foerster, "*Channel Modeling Sub-Committee Report (Final)*," IEEE P802.15-02/490r1-SG3a, 2003. [Google Scholar] [Publisher Link]

[14] Biki Barua et al., "Effect of UWB Channel Delay Parameters on TDOA Localization," *2018 Sixth International Conference on Digital Information, Networking, and Wireless Communications (DINWC)*, Beirut, Lebanon, pp. 32-36, 2018. [CrossRef] [Google Scholar] [Publisher Link]

[15] Aniruddha Chandra et al., "Frequency Domain in Vehicle UWB Channel Modeling," *IEEE Transactions on Vehicular Technology*, vol. 65, no. 6, pp. 3929-3940, 2016. [CrossRef] [Google Scholar] [Publisher Link]

[16] Miodrag Bolic, Majed Rostamian, and Petar M. Djuric, "Proximity Detection with RFID:A Step towards the Internet of Things," *IEEE Pervasive Computing*, vol. 14, no. 2, pp. 70-76, 2015. [CrossRef] [Google Scholar] [Publisher Link]

[17] Guowei Shi, and Ying Ming, "Survey of Indoor Positioning System Based on Ultra Wide Band Technology," *Wireless Communication, Networking and Applications*, pp. 1269-1278, 2015. [CrossRef] [Google Scholar] [Publisher Link]

[18] Guangliang Cheng, "Accurate TOA Based UWB Localization System in Coal Mine Based WSN," *Physics Procedia*, vol. 24, Part A, pp. 534-540, 2012. [CrossRef] [Google Scholar] [Publisher Link]

[19] Bin Xu et al., "High Accuracy TDOA Based Localization Without Time Synchronization," *IEEE Transactions on Parallel and Distributed Systems*, vol. 24, no. 8, pp. 1567-1576, 2013. [CrossRef] [Google Scholar] [Publisher Link]

[20] Chang Liu, Fengshan Bai, and Chunsheng Wu, "A Joint Positioning Algorithm of TDOA and TOF Based on Ultra Wide Band," *Journal of Physics: Conference Series*, vol. 2031, pp. 1-8, 2021. [CrossRef] [Google Scholar] [Publisher Link]

[21] Sven Ole Schmidt, and Horst Hellbrück, "Detection and Identification of Multipath Interference with Adaption of Transmission Band for UWB Transceiver Systems," *International Conference on Indoor Positioning and Indoor Navigation (IPIN)*, vol. 3097, no. 4, pp. 1-16, 2021. [Google Scholar] [Publisher Link]

[22] B.R. Jadhavar, and T.R. Sontakke, "Simulation and Analysis of UWB Indoor Channel through S-V Model for User Location Detection," *International Journal of Computer and Electrical Engineering*, vol. 3, no. 5, pp. 729-738, 2011. [Google Scholar]

[23] Paul Meissner et al., "Analysis of an Indoor UWB Channel for Multipath Aided Localization," *2021 IEEE International Conference on Ultra Wideband*, Bologna, Italy, pp. 565-569, 2011. [CrossRef] [Google Scholar] [Publisher Link]

[24] František Grejták, and Aleš Prokeš, "UWB - Ultra Wideband Charecteristics and the Saleh Valenzuela Modelling," *Acta Electrotechnica et Informetica*, vol. 13, no. 2, pp. 32-38, 2013. [CrossRef] [Google Scholar] [Publisher Link]

[25] Artur Nalobin et al., "Development and Analysis of a Modified Saleh-Valenzuela Channel Model for the UHF Band," *2015 German Microwave Conference*, Nuremberg, Germany, pp. 44-47, 2015. [CrossRef] [Google Scholar] [Publisher Link]

[26] Khadija Hamidoun et al., "UWB System Based on the M-OAM Modulation in IEEE 802.15.3a Channel," *Doctoral Conference on Computing, Electrical and Industrial Systems*, vol. 423, pp. 507-514, 2014. [CrossRef] [Google Scholar] [Publisher Link]

[27] Chadi Abou-Rjeily, "Performance Analysis of UWB System over the IEEE 802.15.3a Channel Model," *IEEE Transactions on Communications*, vol. 59, no. 9, pp. 2377-2382, 2011. [CrossRef] [Google Scholar] [Publisher Link]

[28] Gergely Hollosi, "Distribution of Ultra-Wideband (UWB) Receive Timestamps in Dense Indoor Environment Based on the Saleh-Valenzuela Channel Model," *2022 14th International Conference on Communications (COMM)*, Bucharest, Romania, pp. 1-5, 2022. [CrossRef] [Google Scholar] [Publisher Link]

[29] Changhui Jiang et al., "A UWB Channel Impulse Response De-Noising Method for NLOS/LOS Classification Boosting," *IEEE Communications Letters*, vol. 24, no. 11, pp. 2513-2517, 2020. [CrossRef] [Google Scholar] [Publisher Link]

[30] Asad Saleem et al., "A Critical Review on Channel Modeling: Implementations, Challenges, and Applications," *Electronics*, vol. 12, no. 9, pp. 1-42, 2023. [CrossRef] [Google Scholar] [Publisher Link]

[31] Gergely Hollósi, "Distribution of UWB Receive Time Stamps in Densed Indoor Environment Based on the Saleh-Valenzuela Channel Model," *2022 14th International Conference on Communications (COMM)*, Bucharest, Romania, pp. 1-5, 2022. [CrossRef] [Publisher Link]

[32] Chia-Chin Chong, Youngeil Kim, and Seong-Soo Lee, "A Modified S-V Clustering Channel for the UWB Indoor Residential Environment," *2005 IEEE 61st Vehicular Technology Conference*, Stockholm, Sweden, vol. 1, pp. 58-62, 2005. [CrossRef] [Google Scholar] [Publisher Link]

[33] Zohreh Hajiakhondi-Meybodi et al., "Bluetooth Low Energy Based Angle of Arrival Estimation in the Presence of Rayleigh Fading," *2020 IEEE International Conference on Systems, Man, and Cybernetics (SMC)*, Toronto, Canada, pp. 3395-3400, 2020. [CrossRef] [Google Scholar] [Publisher Link]

[34] Zhuangzhuang Cui et al., "Wideband Air-to-Ground Channel Characterization for Multiple Propagation Environments," *IEEE Antennas and Wireless Propagation Letters*, vol. 19, no. 9, pp. 1634-1638, 2020. [CrossRef] [Google Scholar] [Publisher Link]

[35] Alwin Poulose, and Dong Seog Han, "UWB Indoor Localization Using Deep Learning LSTM Networks," *Applied Sciences*, vol. 10, no. 18, pp. 1-23, 2020. [CrossRef] [Google Scholar] [Publisher Link]